



## Survey of Langmuir and beam-mode waves observed by WHISPER instruments on Cluster spacecraft inside terrestrial foreshock

David Piša<sup>\*(1)</sup>, Ondřej Santolík<sup>(1,2)</sup>, Jan Souček<sup>(1)</sup>

(1) Institute of Atmospheric Physics AS CR, Prague, 14131, Czech Republic, <http://www.ufa.cas.cz>

(2) Faculty Mathematics and Physics, Charles University, Prague, 12116, Czech Republic, <http://www.mff.cuni.cz>

### Abstract

In the upstream region of planetary shocks, intense Langmuir and beam-mode waves are typically observed. Electron beams accelerated at the shock front generate electrostatic waves via beam instability. Waves often occur as narrowband bursts at a frequency close to the local plasma frequency. Broadband emissions at frequencies above and below the plasma frequency are observed deeper in downstream. We present a survey of Langmuir and beam-mode waves in upstream of the terrestrial bow shock from Cluster 2 measurements between years 2002 and 2010. We have used an automated method to identify intense spectral peaks in measured spectra obtained from the WHISPER instrument. Using solar wind data and bow shock positions from OmniWeb, as well as in-situ measurements of interplanetary magnetic field from the fluxgate magnetometer, we have mapped all available observations into foreshock coordinates. We show that the peak intensity increases steeply behind the foreshock boundary and then decreases downstream into the foreshock. We found narrowband emissions at frequencies equal to or above the local plasma frequency in the vicinity of the foreshock boundary. We often detected broadband emissions with the normalized spectral width  $>40\%$  and down-shifted below the plasma frequency deeper inside the foreshock and close to the bow.

### 1. Introduction

Ahead of planetary magnetospheres the supersonic solar wind flow slows down and shapes a collisionless bow shock. Solar wind electrons accelerated at the shock front are reflected back into the solar wind and form electron beams. In regions with these beams, also known as foreshock, the electron distribution becomes unstable and electrostatic Langmuir and beam-mode waves are generated [1]. The processes of generation and evolution of electrostatic waves significantly depend on the solar

wind plasma conditions and generally exhibit complex behavior.

The presence of Langmuir waves has been reported in the upstream region of all planets from Venus to Neptune observed by a number of spacecrafts. The first systematic work was done for Venus' foreshock [3]. Measurements from the Pioneer Venus Orbiter showed the highest wave intensity close to the leading foreshock boundary and strong decrease of the wave intensity for distances beyond  $\sim 15 R_V$  from the tangent point along the foreshock boundary. An extended study of wave activity inside Saturn's foreshock was done from observations of the Cassini spacecraft [4,5] and shows a similar pattern with the highest wave amplitudes close to the sunward foreshock boundary. A survey of the terrestrial foreshock was previously done, for example, by ISEE-3 [6] or Geotail [7] observations. Intense electrostatic wave activity connected to Earth's bow shock was measured at distances up to  $\sim 250 R_E$ , relatively much further than at Venus or Saturn. The difference in Langmuir wave activity inside planetary foreshocks can be explained by the curvature of the shock that significantly controls the energization processes

### 2. Data

For a study of plasma waves outside the terrestrial bow shock, we have used observations of the WHISPER instrument in its burst mode recorded between 2002 and 2010. WHISPER instrument [8] has been designed to measure the electron density determined via the relaxation sounder and the spectrum of natural plasma emissions in the frequency band 2–80 kHz. The total electron density can be obtained from the active mode in a range from 0.25 to  $80 \text{ cm}^{-3}$ . The natural emissions, well measured by the Whisper instrument, can be used for the total electron estimates as well. A combination of an active sounding operation and a passive survey operation provides a time resolution for the absolute electron density determination of 2.2 s in normal mode and 0.3 s in burst mode, respectively.

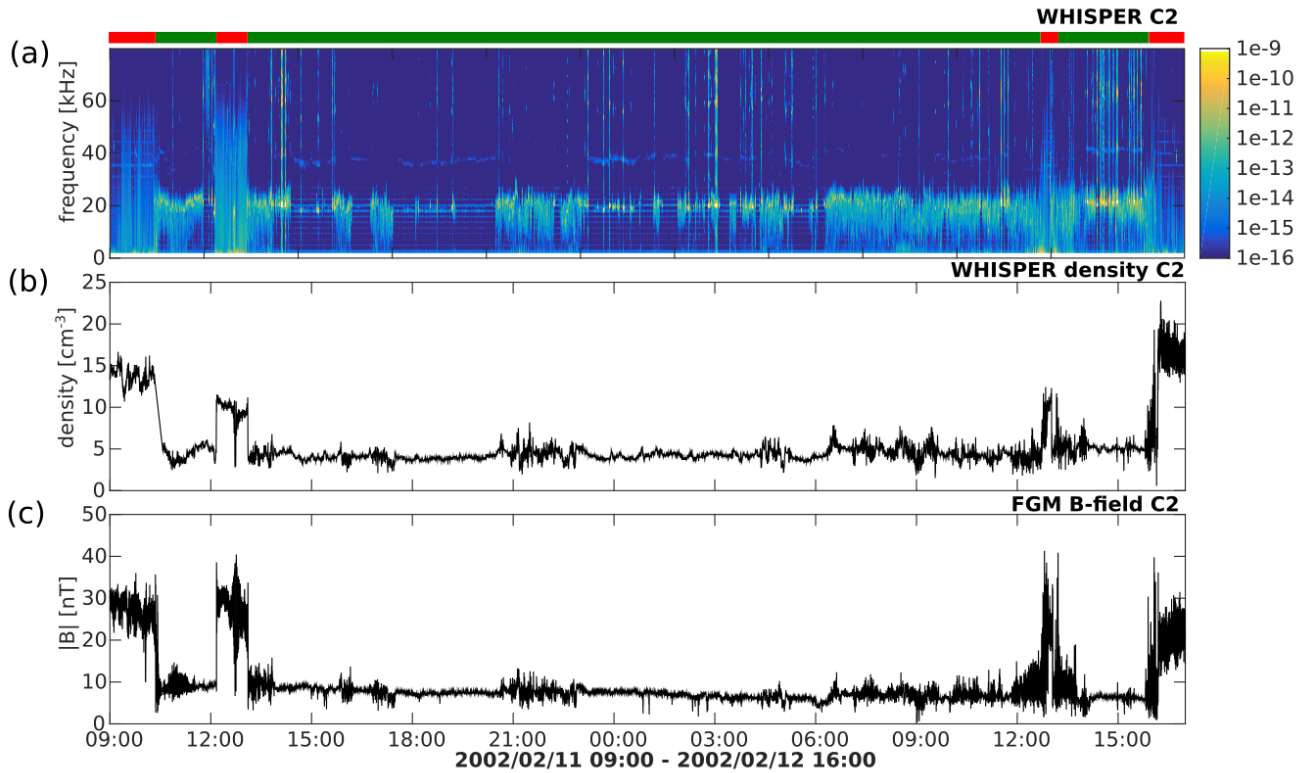


**Figure 1:** Example of CLUSTER 2 measurements in the vicinity of the terrestrial bow shock on 11-12 February 2002. (a) Time-frequency spectrogram of one electric component observed by the WHISPER instrument. Magnetosheath and foreshock visits are labeled by red and green bars, respectively. (b) The local plasma density obtained from the WHISPER measurements. (c) Magnitude of the ambient magnetic field calculated from the Fluxgate magnetometer.

The magnitude and direction of the interplanetary magnetic field (IMF) were obtained from the fluxgate magnetometer (FGM) instrument [9]. Data with a 5 Hz sampling cadence were used and smoothed using a 1 s window to exclude high frequency perturbations that do not contribute to the overall foreshock position and that would cause an inaccurate estimate of the IMF direction. The analyzed data set was restricted to Cluster 2 spacecraft and time periods outside Earth's bow shock. To recognize these positions, we have used the model of the bow shock and solar wind data from OmniWeb (<http://omniweb.gsfc.nasa.gov>). Additionally, we have visually checked all preselected Cluster 2 solar wind visits.

One electric spectrum obtained by the WHISPER receiver has been processed over a bandwidth of 2 – 80 kHz. The WHISPER observations in the burst mode are typically measured with a time and frequency resolutions 0.4 s and 320 Hz, respectively.

Typical observations during the foreshock crossing can be seen in Figure 1 which shows Cluster 2 measurements in the vicinity of the bow shock on 11-12 February 2002. Panel (a) represents the time-frequency spectrogram of the WHISPER observations. Magnetosheath and solar wind regions are labeled on the top by red and green bars, respectively. Panel (b) shows the WHISPER total electron

density. The magnitude of the ambient magnetic field obtained from the FGM instrument is plotted in panel (c). Broadband noise from low frequencies (<10 kHz), higher electron density ( $\sim 15 \text{ cm}^{-3}$ ) and stronger magnetic field ( $>20 \text{ nT}$ ) are observed in the magnetosheath. While inside the foreshock, narrowband emissions around the electron plasma frequency ( $\sim 20 \text{ kHz}$ ), lower density ( $5 \text{ cm}^{-3}$ ), and weaker magnetic field ( $<10 \text{ nT}$ ) are seen.

### 3. Systematic study

All WHISPER natural spectra obtained from 2002 to 2010 during the burst mode intervals were mapped into the foreshock coordinate system. We have used the foreshock coordinate system introduced in [10]. Foreshock's depth (DIFF) is positive along the solar wind flow in the downstream direction measured from the tangent magnetic field line. The DIST coordinate is measured along the tangential field line from the tangent point to the closest point on the tangential field line to the spacecraft position. The sign of the DIST coordinate indicates the downward (-) or duskward (+) sector of the foreshock region. Observations for which the absolute value of the angle between the magnetic field and the

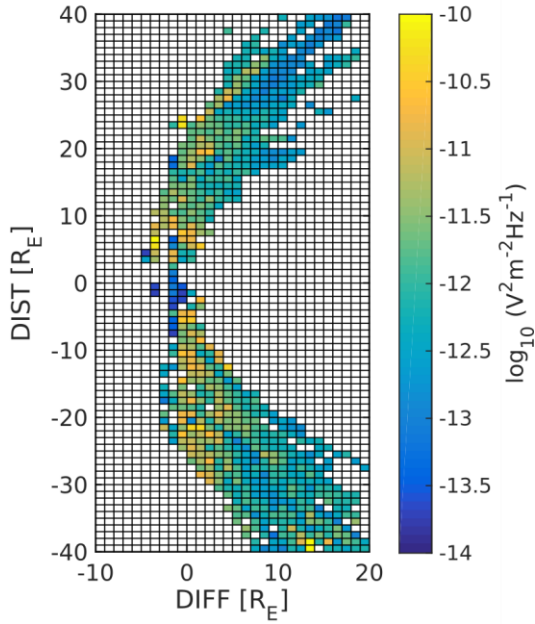


**Figure 2:** Results of the Langmuir and beam-mode wave survey for 2002 through 2010 obtained from C2 WHISPER observations. The average peak intensity as a function of the foreshock position in the  $1 \times 1 R_E$  spatial grid. Only spectra with an intensity  $> 1 \times 10^{-14} \text{ V}^2 \text{ m}^{-2} \text{ Hz}^{-1}$  were analyzed.

direction of the solar wind was lower than 30 or greater than 150 were excluded. Smaller (or larger) angles place the tangent point deep behind the nose of the bow shock, and an unrealistic foreshock position would be obtained. An automated procedure searched for spectral peaks of wave power within the entire WHISPER frequency range for each mapped position. The spectral peak has to have a relative height greater or equal to 2 orders of magnitude (20dB) compared to the background level, in order to be identified. The spectral width is calculated as the peak width at one half of the peak height. Using this method, we have identified almost  $7 \times 10^5$  WHISPER spectra with an intense wave emission.

The results of the Langmuir and beam-mode wave study are shown in Figure 2. The positions are projected into the foreshock coordinates with a spatial grid of  $1 \times 1 R_E$ . Bins with more than 50 events are shown. The wave intensity has a steep increase at the foreshock boundary (DIFF = 0), where the peak intensity reaches  $\sim 1 \times 10^{-10} \text{ V}^2 \text{ m}^{-2} \text{ Hz}^{-1}$ . Deeper into downstream and further from the bow shock, the wave intensity shows a decreasing trend. In front of the foreshock (DIFF < 0) electromagnetic radiation from the foreshock is detected at the intensity level  $10^{-14} \text{ V}^2 \text{ m}^{-2} \text{ Hz}^{-1}$ . One can see higher intensity in front of the foreshock at DIST  $\sim 10 R_E$ . This is possibly caused by an inaccurate foreshock mapping during perturbed solar wind conditions.

The spatial distribution of the normalized spectral widths is plotted in Figure 3. The positions of the WHISPER spectra with an intensity  $> 1 \times 10^{-14} \text{ V}^2 \text{ m}^{-2} \text{ Hz}^{-1}$  are again projected into the foreshock coordinates with a spatial grid of  $1 \times 1 R_E$ . Bins with more than 50 events are shown.

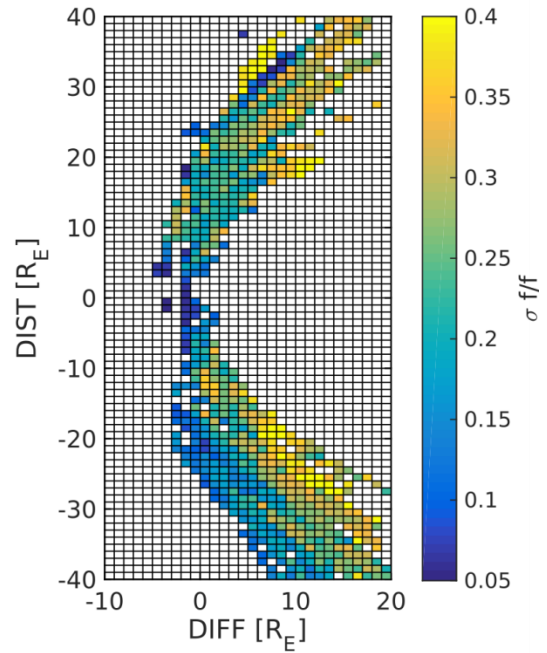


**Figure 3:** Normalized spectral width as a function of foreshock position in the  $1 \times 1 R_E$  spatial grid. Only spectra with an intensity  $> 1 \times 10^{-14} \text{ V}^2 \text{ m}^{-2} \text{ Hz}^{-1}$  were analyzed.

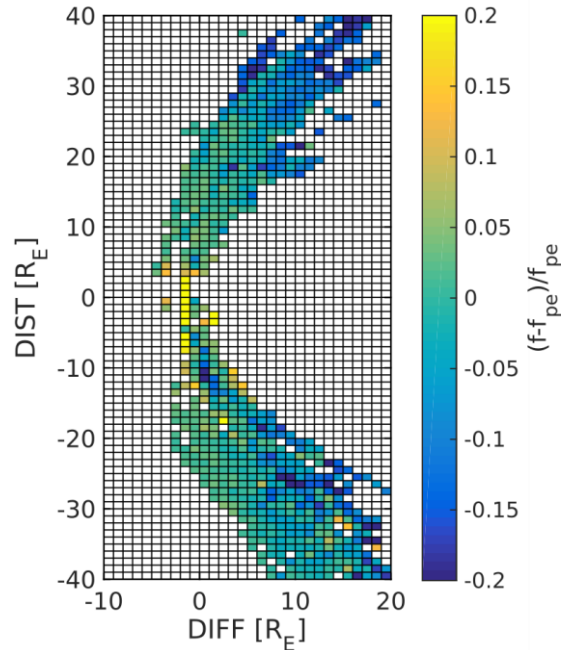


**Figure 4:** Normalized spectral peak deviation from the plasma frequency as a function of foreshock position in the  $1 \times 1 R_E$  spatial grid. Only spectra with an intensity  $> 1 \times 10^{-14} \text{ V}^2 \text{ m}^{-2} \text{ Hz}^{-1}$  were analyzed.

The normalized peak width is calculated for each detected spectra as a ratio of spectral width and peak frequency. Spectra with a narrowband emission (relative width  $\sim 5\%$ ) are observed in the vicinity of the tangent point (DIFF=0 and DIST=0). Broader emissions with the normalized width  $> 30\%$  are observed close to the bow shock and

deeper in the downstream region. Figure 4 shows the normalized spectral peak deviation with respect to the local plasma frequency. In the vicinity of the tangent point, emissions above the plasma frequency are detected. Deeper into the downstream region, we observe emissions, which are downshifted below the plasma frequency.

Observed variations in spectral properties can be explained by changes in the electron distribution function. Deeper inside the foreshock, the beam speed decreases and the beam temperature is higher. This results in a wider frequency range for observed waves. Waves are also more often downshifted with respect to the local plasma frequency [11].

## 4. Summary

This study focuses on the spatial and spectral properties of Langmuir and beam-mode waves inside the terrestrial foreshock. Using a long term survey from 2002 to 2010, we have analyzed all available WHISPER spectra obtained inside the upstream region. We detected almost  $7 \times 10^5$  spectra with intense emissions in the burst mode for a frequency range of 2–80 kHz.

The wave activity increases steeply behind the foreshock boundary (DIFF=0). Deeper in the foreshock and further from the bow shock the wave intensity decreases. Narrowband spectra with a relative peak width of ~5% are observed in a region behind the leading foreshock boundary, while broader emissions with relative widths >40% are seen deeper inside the foreshock and closer to the bow shock. In a relatively narrow region behind the leading foreshock boundary, the most intense spectral peaks are observed above the local plasma frequency. Deeper downstream, the spectral peaks are more often downshifted below the plasma frequency.

## 6. Acknowledgements

We thank the WHISPER and FGM teams for scientific data. Data are accessible through the Cluster Science Archive (<https://www.cosmos.esa.int/web/csa>) and OmniWeb (<http://omniweb.gsfc.nasa.gov>). This work has been supported from grants 16-16050Y of the Grant Agency of Czech Republic and Praemium Academiae award.

## 7. References

[1] F. L. Scarf, R. W. Fredricks, L. A. Frank, and M. Neugebauer (1971), Nonthermal electrons and high-frequency waves in the upstream solar wind, 1. Observations, *J. Geophys. Res.*, 76, 5162–5171, doi:10.1029/JA076i022p05162.

[2] S. A. Fuselier, D. A. Gurnett, and R. J. Fitzenreiter (1985), The downshift of electron plasma oscillations in the electron foreshock region, *J. Geophys. Res.*, 90, 3935–3946, doi:10.1029/JA090iA05p03935.

[3] G. K. Crawford, R. J. Strangeway, and C. T. Russell (1993), VLF imaging of the Venus foreshock, *Geo. Res. Lett.*, 20, 2801–2804, doi:10.1029/93GL01258.

[4] D. Piša, G. B. Hospodarsky, W. S. Kurth, O. Santolík, J. Souček, D. A. Gurnett, A. Masters, and M. E. Hill (2015), Statistics of Langmuir wave amplitudes observed inside Saturn's foreshock by the Cassini spacecraft, *J. Geophys. Res. Space Physics*, 120, doi:10.1002/2014JA020560.

[5] D. Piša, O. Santolík, G. B. Hospodarsky, W. S. Kurth, D. A. Gurnett, and J. Souček (2016), Spatial distribution of Langmuir waves observed upstream of Saturn's bow shock by Cassini, *J. Geophys. Res. Space Physics*, 121, doi:10.1002/2016JA022912.

[6] J. Fitzenreiter (1995), The electron foreshock, *Adv. Space Res.*, 15, 9–27, doi:10.1016/0273-1177(94)00081-B.

[7] Y. Kasaba, H. Matsumoto, Y. Omura, R. R. Anderson, T. Mukai, Y. Saito, T. Yamamoto, and S. Kokubun (2000), Statistical studies of plasma waves and backstreaming electrons in the terrestrial electron foreshock observed by Geotail, *J. Geophys. Res.*, 105(A1), 79–103, doi:10.1029/1999JA900408.

[8] P. M. Decreau et al., (2001) Early results from the Whisper instrument on Cluster: An overview. In: *Annales Geophysicae*, Vol. 19, No. 10-12, 2001, p. 1241-1258.R.

[9] A. Balogh et al., (2001) The Cluster Magnetic Field Investigation: overview of in-flight performance and initial results. In: *Annales Geophysicae*, Vol. 19, No. 10-12, 2001, p. 1207-1217.R.

[10] P. C. Filbert, and P. J. Kellogg (1979), Electrostatic noise at the plasma frequency beyond the Earth's bow shock, *J. Geophys. Res.*, 84, 1369–1381, doi:10.1029/JA084iA04p01369.

[11] I. H. Cairns (1989), Electrostatic wave generation above and below the plasma frequency by electron beams, *Phys. Fluids B*, 1(1), 204–213, doi:10.1063/1.859088.